Performance of Silicon Pore Optics

Maximilien J. Collon[1], Ramses Günther[1], Marcelo Ackermann[1],
E. J. Buis[2], G. Vacanti[2] Marco W. Beijersbergen[1],
Marcos Bavdaz[3], Kotska Wallace[3], Michael Freyberg[4], Michael Krumrey[5]

[1] cosine Research B.V, Niels Bohrweg 11, NL-2333 CA Leiden,
(tel) +31 71 528 49 62, (fax) +31 71 528 59 63, m.collon@cosine.nl

[2] cosine Science & Computing B.V, Niels Bohrweg 11, NL-2333 CA Leiden,
(tel) +31 71 528 49 62, (fax) +31 71 528 59 63, g.vacanti@cosine.nl

[3] European Space Agency, ESTEC, Keplerlaan 1, PO Box 299, 2200 AG Noordwijk, The Netherlands,
(tel) +31 71 565 4933, (fax) +31 71 565 4690, marcos.Bavdaz@esa.int

[4] Max-Planck-Institut für extraterrestrische Physik, Giessenbachstrasse, 85748 Garching, Germany,
(tel) +49 89 300 00 3849, (fax) +49 89 300 00 3569, mjf@mpe.mpg.de

[5] Physikalisch-Technische Bundesanstalt, Abbestr. 2-12, 10587 Berlin, Germany,
(tel) +49 30 6392-5085, (fax) +49 30 6392-5082, Michael.Krumrey@ptb.de

Abstract:

Silicon pore optics have been developed over the last years to enable future astrophysical X-ray telescopes and have now become a candidate mirror technology for the XEUS mission. Scientific requirements demand an angular resolution better than 5" and a large effective area of several square meters at photon energies of 1 keV. This paper discusses the performance of the latest generation of these novel light, stiff and modular X-ray optics, based on ribbed plates made from commercial high grade 12" silicon wafers. Stacks with several tens of silicon plates have been assembled in the course of an ESA technology development program, by bending the plates into accurate shape and directly bonding them on top of each other. Several mirror modules, using two stacks each, have been aligned and integrated to form the conical approximation of a Wolter-I design. This paper presents the status of the technology, addresses and discusses a number of activities in the ongoing ESA technology development and shows latest results of full area measurements at the MPE X-ray test facility (PANTER).

Keywords: X-ray optics, X-ray astronomy, silicon, wafer, stack, pore optics, X-ray telescopes

1. INTRODUCTION

One way of building imaging X-ray telescopes that achieve large collecting area and high angular resolution is to use double (Fresnel) reflection of a parabolic and a hyperbolic mirror surface under grazing incidence angles, a so-called Wolter-I optic. Future X-ray telescopes like e.g. XEUS [1] shall observe in an energy band of 0.1 to 10 keV. To achieve high reflectivity of the mirror surfaces at these energies requires a high-Z material and/or a (multi-layer) coating, an rms surface roughness significantly better than 1 nm and a long focal length of 35 to 50 m. Shorter focal lengths or higher surface roughness will reduce the high energy response.

A telescope with an effective area of 5 m^2 at 1 keV and with a focal length of 35 m will then require about 1350 m^2 of super polished mirror area and will have a diameter of about 4.5 m. A technology based on mounting many replicated nickel shells, as was used for XMM-Newton [2], is not suited because of the mass limitation imposed by the launch vehicle and because of the high angular resolution requirement, which is difficult to achieve when aligning and fixing individual mirror shells into a spider wheel. One candidate technology is slumped glass [3 - 5], which has been demonstrated to achieve the desired angular resolution on individual mirror plates, but to our knowledge it has not yet been demonstrated that it is possible to mount many shells into larger assemblies whilst maintaining the angular resolution.

Space Telescopes and Instrumentation 2008: Ultraviolet to Gamma Ray, edited by Martin J. L. Turner,
Kathryn A. Flanagan, Proc. of SPIE Vol. 7011, 70111E, (2008) · 0277-786X/08/$18 · doi: 10.1117/12.789723

Silicon pore optics have been developed by ESA to enable future large X-ray telescopes with several square meters of collecting area whilst achieving an angular resolution of several arc seconds. The development started in 1998 with the conceptual idea of using super-polished 12" silicon wafers as reflecting surfaces for X-rays [6 - 9]. These wafers are 0.8 mm thin, have the required surface roughness of 0.1 nm measured on AFM length scales and have a plan-parallelism better than 0.5 mm measured over 300 mm. At the same time one has to nest the curved shells very closely together in order to achieve a high aperture utilisation. This requires a mounting mechanism to individually fix the shells into the required position. The idea was to thin the silicon wafers on at least 80% of the area down to 150 μm and to leave a number of ribs with a width of about ~0.2 mm. These ribs can be used to interconnect the shells and act as stiffeners in longitudinal direction. There are then multiple methods of bonding these ribbed plates together. In our case we directly bond two silicon plates together [10, 11]. The stacking process (shown in Figure 1) has been developed by cosine Research and partners from 2001 to 2005 and has been discussed in detail in [12 - 15].

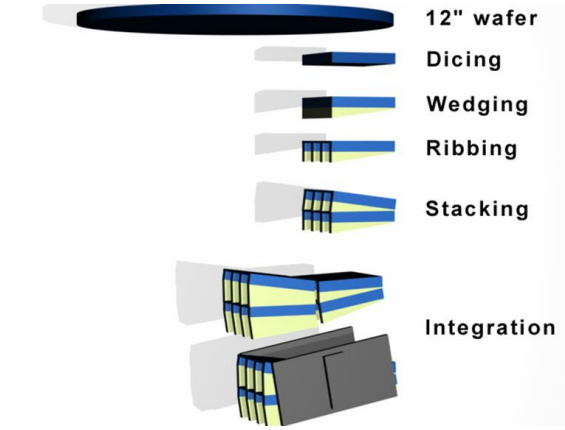

Figure 1: Process flow for the manufacture and assembly of silicon pore optics, starting from the 12" wafer. The end product is a mirror module, consisting of two silicon stacks with up to 100 plates, co-aligned with arc-second accuracy and fixed by two mounting brackets.

From 2005 to 2007 a dedicated project was run by ESA to demonstrate the entire production chain from wafer level, over plate and stack manufacturing to mirror module integration up to the petal level. The petal is a radial segment of the telescope, into which the mirror modules are then integrated. A significant effort went into the development of wedged plates. Wedged plates are required to build true focussing optics by tilting every plate at an angle given by the geometry of a Wolter-I optic. The wedge angle depends only on the focal length and the plate thickness and is very small ($\sim 3.8\times10^{-6}$ rad for the parabolic stack and 11.6×10^{-6} rad for the hyperbolic stack at a focal length of 35 m), resulting in a maximum height difference of ~1 μm over the length of a silicon plate for the outer radius of 2 m and ~4 μm for an inner radius of 0.5 m. Any method to achieve such a wedge will affect the bonding process and the accuracy of the wedge angle will directly influence the PSF.

The ESA Technology Reference Programme project was completed successfully [16] and the entire production chain was demonstrated up to petal level. This meant that one could now concentrate on the most critical element of silicon pore optics: the stack. A new project has been started in Oct 2007, which concentrates entirely on improving the quality of the stacks by further automation of the assembly process, on developing coating methods and on optimising the plate geometry to maximise the bond strength.

2. STATUS

We have demonstrated [16] that it is possible to assemble stacks of 35 plates and to align them into mirror modules with arc-second accuracy. We have built several uncoated mirror modules and integrated them into a petal, which has been tested at PANTER. In this chapter we discuss results of effective area measurements and of the first mirror module made from wedged plates.

2.1 Effective area

We have performed at PANTER effective area measurements on one of the uncoated mirror modules (see Table 1), which consisted of 35 plates. The measured effective area is about 93% of the expected effective area at photon energies up to 1.5 keV, taking into account known geometric effects and the reflectivity of bare SiO_2 with a surface roughness of 0.5 nm. The missing 7% is attributed to small relative alignment errors between the two stacks and to the fact that modelling the surface with a constant thickness SiO_2 layer is not an accurate representation of the reflecting surface composition. At higher energies of 3 keV we obtain 70% of the expected effective area, which could be explained by an increased roughness due to multiple re-use of the sample plates that were finally stacked. However, at 4.5 keV we obtain a significantly higher effective area than expected. This could be attributed to unidentified scattering in the experimental setup. Both results indicate that additional effort will be required in modelling the reflecting surface and that further investigation is required. These measurements will be repeated when coated plates become available.

Table 1 Measured and expected effective area of XOU-3

Energy	**eV**	***280***	***1490***	***2980***	***4510***
Reflectivity SiO_2 @ 0.5 nm (rms)		0.923	0.918	0.439	0.021
Expected effective area	mm^2	883	874	200	0
Measured effective area	mm^2	826	814	140	8
Measured / expected		0.94	0.93	0.70	

2.2 Wedged plates

The development of the wedging process was completed in July 2007. Since then we have been able to assemble a stack made of wedged plates that has been tested in the laboratory of the Physikalisch-Technische Bundesanstalt (PTB) at BESSY II and at the MPE PANTER facilities. Neither facility has yet been upgraded to allow one to measure the mirror modules at the right focal distance (50m). At BESSY it is possible to place a detector 5 m from the stack, while at PANTER this distance is 8 m. At BESSY one can use pencil beams to sample the entire area of a mirror module. This has the advantage of a well collimated 50 μm beam, representing a source at infinity, which allows predicting the performance at other distances then the measured one [16]. The drawback is that one can not determine the absolute efficiency of the optics.

PANTER allows measuring the effective area, however the source (at a distance of 123 m) can not be considered at infinity because it is not very long compared to the focal length of the optic. We therefore have to consider the beam divergence when analysing the focusing properties of the mirror module. In double reflection a divergent beam first reflects off the first stack of mirrors. These mirrors transform the beam with a divergence angle γ into a convergent one, as shown in Figure 2. As the geometry of the second set of mirrors is identical to the first ones, the reverse effect is observed; the sign of γ changes and its magnitude is conserved. The outgoing beam is hence equally divergent to the original incoming beam, which partially compensates for the radial focusing introduced by the wedge angle of the plates.

Based on the thin lens equation, one can calculate that for an optic with a focal length of 35 m and a source distance of 123 m the real focus is located at a distance of 48.8 m. For a 50 m optics, which is still the baseline for the technology development due to exisiting equipment considerations, the focus is found at 84 m. Taking this into account yields that one would expect to observe at PANTER, at a distance of 8 m from the optics, a plate spacing of 711.5 μm if the plates have the correct wedge angles. MPE has measured (see Figure 3) a plate pitch of 713 μm, which is within the measurement accuracy and in very good agreement with the expected focusing properties. This means that for the first time we have demonstrated a fully focusing lens element made from silicon pore optics.

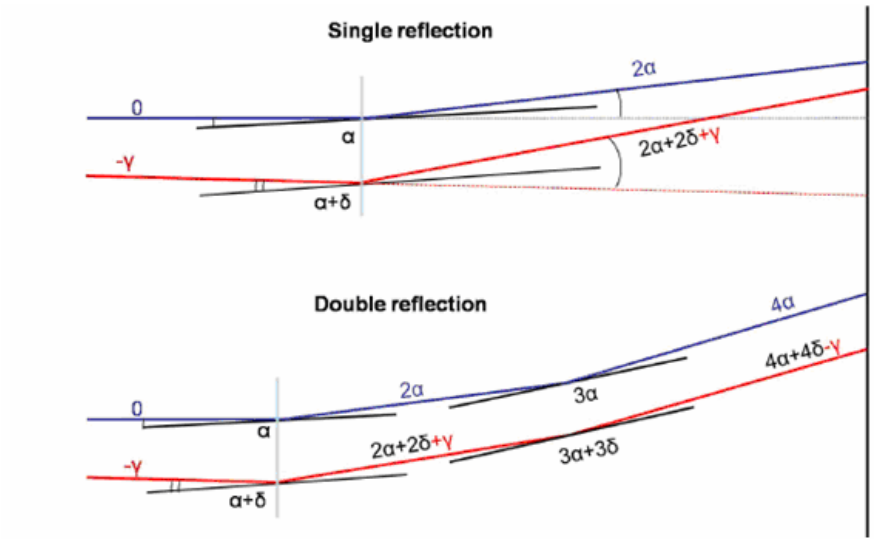

Figure 2: The effect of a divergent beam with divergence angle γ reflecting off a set of mirror plates oriented at an angle α to the beam and having a wedge angle δ. In single reflection (top), the mirrors convert the beam with divergence γ into a convergent beam. A set of two consecutive mirrors (bottom) however does not alter the divergence of the beam.

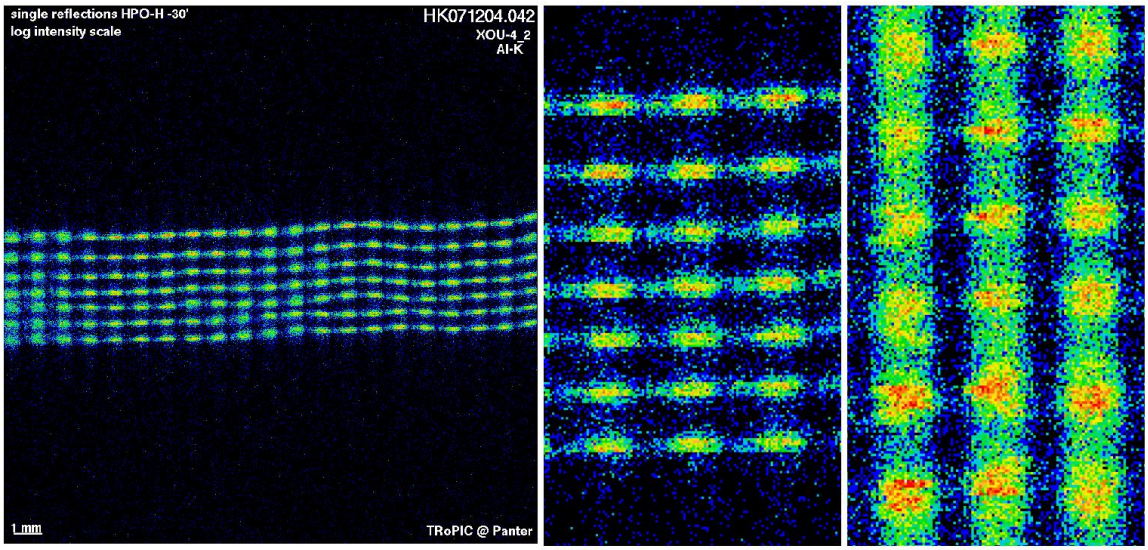

Figure 3: The wedged mirror module measured at PANTER at an energy of 1.49 keV at a distance of 8 m from the optics, using the new TRoPIC CCD. Single reflections are shown on the left and a zoomed part of several mm is shown in the centre. The results are compatible with measurements at BESSY, which gives a HEW of about 17" [16]. On the right one observes the same area as in the centre, but in double reflection. Note that the bottom five plates are wedged and the top three are unwedged; One can clearly observe the difference in the plate pitch. In single reflection the spacing of the pore decreases due to the divergence of the beam (see Figure 2). The PANTER measurements of the double reflected beam (right) prove, within the measurements accuracy, the plates have the correct wedge angles. This demonstrates for the first time a true focusing optics made from silicon pore optics.

3. TECHNOLOGY DEVELOPMENT

3.1 Roadmap

Silicon Pore optics technology has to reach a technology readiness level (TRL) of 5 over the next 4 years to be compliant with the current ESA Cosmic Vision 2015-2015 scientific program schedule. A TRL 5 requires demonstrating that a fully coated mirror module can achieve 5" angular resolution in a relevant (cold) environment and be compatible with launch conditions. Up to mirror module level this requires technology development in areas that have so far only been touched upon (i.e. coating, annealing of stacks, fabrication of inner radii mirror modules, environmental testing, baffling) and improvements in the quality of stacks (process automation, particle detection and removal systems, metrology improvement). In addition one has to reduce the cost per ribbed and wedged plate and one has to start developing mass production robots. This chapter discusses current developments in the areas of stacking, metrology, coating and performance prediction.

3.2 Stacking process development

The manufacturing of silicon pore optics is currently done at cosine in a class 10 cleanroom. The stacking of ribbed and wedged silicon plates is completely automated with a dedicated robot. [10]. This robot is capable of extracting previously cleaned plates from a container, of inspecting them using high resolution cameras, of aligning them with micro-meter accuracy, of bending the plates into shape, of bonding them and of inspecting the stack with interferometric means. This second generation robot has been used over the last years to assemble the first mirror modules. It has, however, several limitations which necessitate the development of a third generation stacking robot.

To improve on the figure of the silicon pore requires fully automated detection and removal of sub-micrometer particles, which could become trapped in between two bonding surfaces. These particles originate from the transport of plates and from the manual plate cleaning process. Consequently created figure distortions can become orders of magnitude larger than the actual size of the particle itself. Therefore, it is imperative to remove these particles completely from any bonding surface. Particle removal is a hot topic in wafer industry, however they are dealing with round wafers with rounded corners. In our case, however, we have rectangular plates with sharp ribs, which means that standard particle detection and removal equipment can not be used.
cosine is developing a dedicated particle detection system to determine the effectiveness of particle removal and to pre-select plates before they are stacked. This particle detection system is based on scattered light detection in combination with advanced image analysis and can analyse an entire plate of 66×66 mm^2 within one minute. The system is being tested at the time of writing of this paper and first results indicate that resolving at least 500 nm sized particles on both the reflective and the ribbed side of the plates (see Figure 4) is possible.

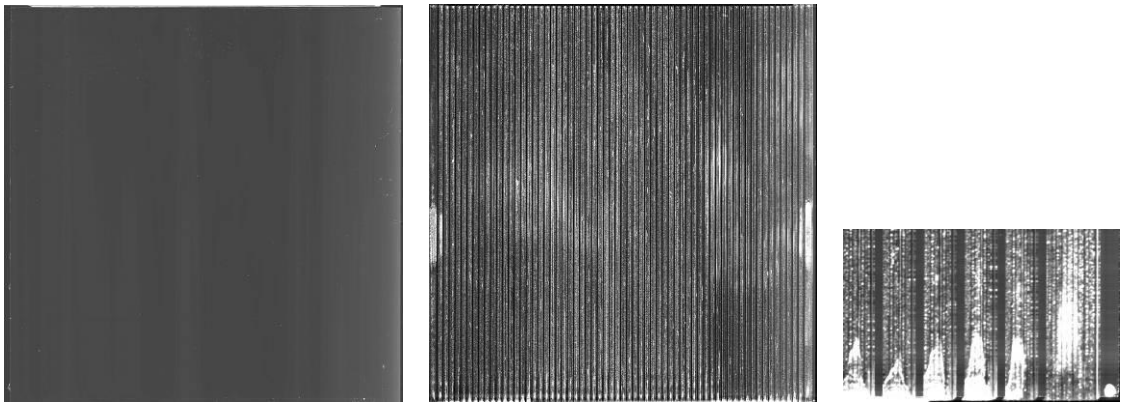

Figure 4: Left Image: High resolution scan of the reflective side of a plate. Middle image: ribbed side. Right image: a close up view of the right bottom corner of the middle image. The dark vertical stripes are the bonding surfaces of the ribs.

With this system it is possible to measure the distribution and size of the remaining particles and the exact location of the particle. This is used in combination with an automated particle removal system. However, the most efficient method is to avoid particulate contamination of the plates down to a size of 100 nm before they are being stacked. cosine's approach to achieve this involves a combination of wet and dry cleaning technology adapted to the cleaning of square plates.
Once the plate is free of particles it will be activated using a dry process. This new dry plate activation process enhances the surface energy without increasing the surface roughness and will also be beneficial for handling coated plates. For maximum flexibility, easy operation and cleanliness of the system a six degree of freedom robotic arm has been added to the stacking robot. This robotic arm acts as the centre of the stacking system, which thereby gets a circular and modular geometry, instead of the linear topology used so far. The robotic arm transfers the plate towards the cleaning, inspection and assembly locations, which are now decoupled from each other.
Furthermore, we are carrying out annealing experiments that increase the bond strength by a factor of 10 and turn the van-der-Waals bonds into permanent covalent bonds. cosine will carry out bond strength measurements in the near future to study different plate geometries and annealing parameters in preparation for future environmental tests. First experiments with stacking plates at inner radii of 0.5 m (so far the technology development has concentrated on a radius of 2 m) will be carried out as well.

3.3 Metrology

In the process of upgrading the stacking robot we are also further developing the metrology equipment. We have managed to perform an X-ray performance prediction starting from interferograms that we record of every plate when it is being stacked. From this we derive the slope errors which we can use to predict the PSF of the optics. At BESSY we then use pencil beam to sample the stack with high spatial resolution. From the position of the reflected beam and from its spread we can derive the local slope errors. In addition, since we measure where the beam enters the stack and where the reflected beam hits the detector we can use this information to perform X-ray tracing and predict the PSF at other focal lengths [16].

The surface roughness of the Si mirror plates has been measured with different surface measurement techniques. We have performed AFM, Chapman profiling, X-ray reflectivity and interferometry measurements.

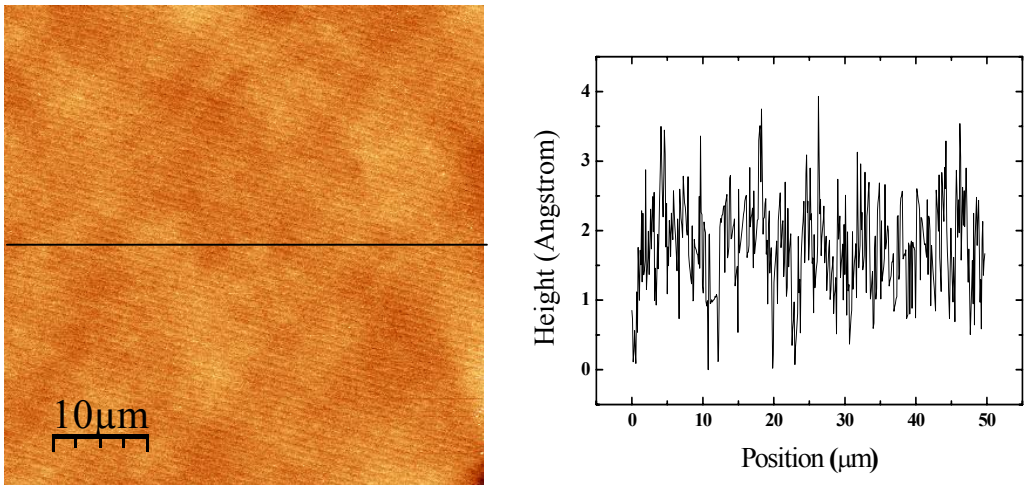

Figure 5: AFM measurement of the reflective side of an uncoated silicon plate as it typically is used for stacking. The right plot shows the height variation along a horizontal cross section. On length scales up to 50 µm the rms roughness is 0.67 Å. The regular pattern visible in the image is 50 Hz noise.

These techniques are sensitive to changes in surface height (i.e. roughness) on different length scales. By using several different techniques, we are able to determine the surface roughness on a length scale ranging from nanometres up to tens of centimetres (8 orders of magnitude). We then perform a Fourier Transform (FT) to convert this data into spatial frequency components. The data from the FT is presented as the Power Spectral Density (PSD) of the surface roughness. By representing the data in this way, we can easily compare the results from the different techniques. The overlapping

ranges in wavelength of the different techniques show the same power, making this set of measurements self-consistent. With this PSD we can assess every frequency range separately, relatively independently of the measurement technique. At the time of writing this paper we are concluding a measurement campaign to characterise on length scales from cm to nm the surface of the silicon plates as a function of processing steps.

Figure 5 shows an AFM measurement of a silicon plate before ribbing. The rms roughness is better than 0.1 nm on length scales up to 50 μm. After all processing steps, using the old wet chemical process known to slightly roughen the surface, we have measured [16] in X-rays at 8 keV an rms roughness of 0.47 nm. By using the new dry surface activation process we expect this to significantly improve.

3.4 Performance prediction

Detailed performance simulations of the pore optics are necessary in order to understand the measurement data of the X-ray campaigns and to correlate the results back to the development programme. We have therefore embarked on a software development effort to insure that all metrology data at our disposal can be modelled and ray traced, and the results compared with the measurements taken at X-ray facilities.

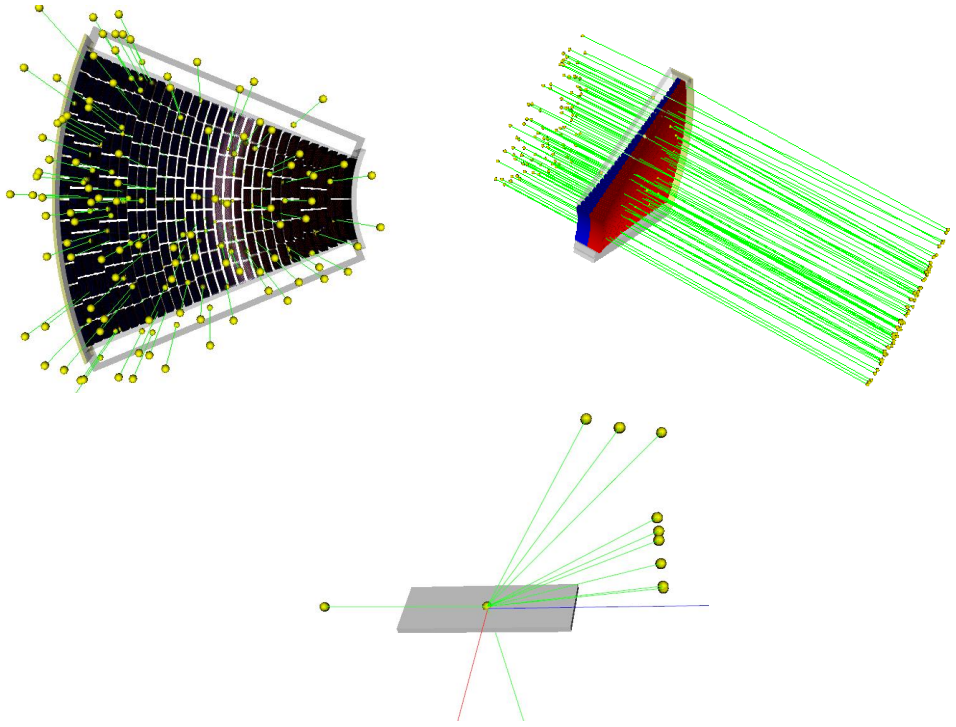

Figure 6: Top left: Detailed raytracer model of a XEUS petal, where each element (plates, ribs, spacers, and wedges) are individually modelled. Top right: X-rays enter from the left and are reflected and scattered off the individual mirror surfaces. Bottom: Visualization of a pencil beam experiment. X-ray photons are coming from the left, and are scattered after reflection on the surface of a silicon plate. Note that the surface figure errors have been included directly from the interferogram measured with the stacking robot metrology system. The surface roughness is modelled according to the PSD measured with AFM and X-ray reflectometry. Scattering angles are enhanced for clarity.

The development leverages the Geant4 simulation toolkit [17, 18]. This is a large library of C++ code, developed by CERN in order to support the Large Hadron Collider. The toolkit is able to track any kind of particle through large geometries, by taking into account all of the relevant physical processes: it constitutes a solid foundation upon which a raytracer for X-ray optics can be built. In our development we have tackled two main sets of issues: make Geant4 aware

of the physical processes describing the reflection and scattering of X-ray photons at grazing angles; exploit the detailed surface metrology data at our disposal to modify the surface normals at the place where an X-ray photons strikes a surface.

The physics of X-ray reflection and scattering has been implemented to describe the standard Fresnel reflection and scattering on bulk surfaces, surfaces with an overcoat, and surfaces with a multilayer coating. The optical performance of the optics depends on a number of surface properties that we are able to measure in the lab: the surface roughness, the power density distribution of the surface profile, and the detailed interferogram of the surface of each plate. Our simulator is able to absorb the different metrological data and use them for detailed raytracing. In particular, in our simulations we can use the interferograms of the silicon plates as textures for our geometrical models of the optics, so that the simulator can be used to predict the results of X-ray pencil beam illumination tests. At the moment of writing this paper the software development is almost complete, and we have started comparing simulations with data.

Our code can also be used to predict the performance of the complete XEUS optic under a number of different assumptions (see Figure 6). We have built detailed models of the stacks, where each element (plates, ribs, spacers, and wedges) are individually modelled. We are therefore able to predict the final optical performance based on assumed production errors and misalignments of all these components. This predictive capability can be turned around, and used to set the maximum production errors and misalignments allowed by the target final resolution. This functionality is currently being used to derive an error budget for manufacturing the mirror modules optics.

3.5 Coating

We have reported on initial trials to coat the silicon plates [16] and we have now set up, together with the Danish Space Institute, a dedicated programme to develop masked coated silicon plates. Several different materials, for example Iridium, will be tried out in combination with carbon overcoatings [19] to enhance the reflectivity around the iridium absorption edge at 1.8 keV. The goal of the coating development is to investigate two different scenarios. The first one is to mask the Si surface before the coating process in order to leave bare silicon at the positions where the bonding will take place. Only a marginal loss of reflective surface is expected with this method, as the uncoated parts are those that would not in any case contribute to the reflectivity of an uncoated HPO. Only a very small area around the bondable parts is left uncoated as a safety margin and will show a loss in reflectivity. Another option being considered is to overcoat the Ir or C layer with Si, and to directly bond on top of that Si layer. In this option the loss in reflectivity will be determined by the thickness of Si needed for the bonding and the surface roughness of this Si layer. Both reflectivity and bond tests are being performed on both types of coated plates (masked and Si overcoated). More extensive results on the reflectivity of coated Si samples are present in the paper by *D.H. Lumb et al* (SPIE proceedings 2008).

4. CONCLUSIONS

The technology development for silicon pore optics has successfully demonstrated the entire prototype production chain from wafer level up to mounted optics integrated into a petal and tested at PANTER. We have shown in this paper that wedged plates have been stacked and that a focussing optic made from silicon pore optics has been successfully tested. The effective area of the uncoated mirror modules, at energies up to 1.5 keV, reaches 93% of the expected effective area. The surface roughness of the silicon plates before processing is 0.1 nm, on length scales up to 50 μm, and reaches 0.47 nm after all processing steps, measured in X-rays at 8 keV. The development effort now concentrates on improving the figure of the stacks, which shall be achieved by further automation of the stacking process. We have closed the metrology loop by developing an X-ray tracer capable of modelling the entire XEUS optics, taking into account metrology data from the stacking systems. We have also begun to address new issues: masked coating of the plates, bond strength measurements and preparation for environmental testing. All of these activities should result in reaching a TRL of 4 over the next two years and a TRL of 5 over the next four years.

5. REFERENCES

[1] A Parmar, G Hasinger and M Turner, "XEUS - the X-ray Evolving Universe Spectroscopy Mission", Proc 34th Cospar Assembly, 2368 (2004).

[2] Jansen, F. et al., "XMM-Newton observatory", Astron. Astrophys. 365, L1-L6 (2001).

[3] P. Friedrich, et al., "Manufacturing of Wolter-I mirror segments with slumped glass", Proc. SPIE 6266, 62661G (2006).

[4] O. Citterio, et al., "Optics for EUV, X-Ray, and Gamma-Ray Astronomy", Proc. SPIE 5168, 180 (2004).

[5] W. Zhang et al, "Development of Lightweight X-Ray Mirrors for the Constellation-X Mission", Proc. SPIE 6688, 668811 (2007).

[6] Bavdaz, M. et al., "Progress at ESA on high-energy optics technologies", Proc. SPIE 5168, 136-147 (2004).

[7] Beijersbergen, M. et al., "Development of x-ray pore optics: novel high-resolution silicon millipore optics for XEUS and ultralow mass glass micropore optics for imaging and timing", Proc. SPIE 5539, 104-115 (2004).

[8] Beijersbergen, M. et al., "Silicon pore optics: novel lightweight high-resolution X-ray optics developed for XEUS", Proc. SPIE 5488, 868-874 (2004).

[9] Kraft, S. et al., "Development of modular high-performance pore optics for the XEUS x-ray telescope", Proc. SPIE 5900, 297-308 (2005).

[10] Günther, R. et al., "Production of silicon pore optics", Proc. SPIE 6266, 626619 (2006).

[11] Collon, M. J. et al., "Metrology, integration, and performance verification of silicon pore optics in Wolter-I configuration", Proc. SPIE 6266, 626618 (2006).

[12] Collon, M. J. et al., "Performance characterization of silicon pore optics", Proc. SPIE 6266, 62661T (2006).

[13] Freyberg, M. et al., "Potential of the PANTER x-ray test facility for calibration of instrumentation for XEUS", Proc. SPIE 6266, 62663H (2006).

[14] Graue, R. et al., "Assembling silicon pore optics into a modular structure", Proc. SPIE 6266, 62661U (2006).

[15] Kraft, S. et al., "Programmatics of large scale production of silicon pore optics for future x-ray telescopes", Proc. SPIE 6266, 626617 (2006).

[16] Collon, M. J. et al., "Silicon pore optics for astrophysical x-ray missions", Proc. SPIE 6688, 668813 (2007).

[17] Agostinelli, S., et al., "G4-a simulation toolkit", Nuclear Instruments and Methods in Physics Research A 506, 250-303 (2003).

[18] Allison, J., et al., " Geant4 developments and applications", IEEE Transactions on Nuclear Science 53 No. 1, 270-278 (2006).

[19] D. H. Lumb, F.E. Christensen, C.P. Jensen and M. Krumrey, “Influence of a carbon over-coat on the X-ray reflectance of XEUS mirrors”, Opt. Commun. 279, 101 – 105 (2007).